JOURNAL OF OPTOELECTRONICS AND ADVANCED MATERIALS Vol. 10, No. 5, May 2008, p. 1103 - 1105

Theoretical and experimental analysis of laminated iron core losses

P. G. ROVOLIS*, A. G. KLADAS
Laboratory of Electrical Machines, Electric Power Division, Faculty of Electrical and Computer Engineering, National Technical University of Athens, 9 Heroon Polytechneiou Street, Athens 15780, Greece

Iron loss analysis constitutes an important factor in transformer and electrical machine design. Especially, operation under distorted grid voltage waveforms and variable speed motors supplied by inverters presents increased iron losses due to harmonic frequencies. The paper presents a methodology for determination of harmonic iron losses in laminated iron cores under sinusoidal excitation. The method is based on a convenient modification of Jiles-Atherton model enabling to account for dynamic effects. The model tuning is performed by using measured hysteresis loops in iron laminations for sinusoidal excitation of various frequencies in Epstein device.

(Received March 13, 2008; accepted May 5, 2008)

Keywords: Electrical machine, Laminated iron core losses, Estein device

1. Introduction

Static Jiles-Atherton [1] and Preisach models [2] enable accurate representation of magnetic hysteresis in iron laminations, in the low frequency range, by using parameters derived from experimental data [3], [4], [6]. However, for frequencies greater than 100 Hz, such models need appropriate modifications [3], [5]. These changes involve consideration of the main stages of magnetization in ferromagnetic initial reversible magnetization, rapid irreversible magnetization and the slow approach to saturation [7].

A classical description of the process is given by the Langevin function with the Weiss correction. Therefore, most hysteresis models need additional, physical or mathematical, assumptions determining more accurately the influence of the external field frequency on the magnetic domains inside a ferromagnetic material and formation of the loops. The shapes of obtained loops provide acceptable accuracy when compared to measured ones by the Epstein device, for sinusoidal external field time variation.

2. Methodology

In the literature convenient modifications of Jiles-Atherton models [1] are proposed in order to include dynamic effects [2]. The equation of hysteresis is most simply represented in the form of its two components.

The reversible and irreversible susceptibilities expressed as follows [4]:

$$\frac{dM_{irr}}{dH} = \frac{M_{an} - M_{irr}}{\delta\kappa - \alpha(M_{an} - M_{irr})} \tag{1}$$

$$\frac{dM_{rev}}{dH} = c\left(\frac{dM_{an}}{dH} - \frac{dM_{irr}}{dH}\right) \tag{2}$$

where M_{irr} denotes the magnetization irreversible, M_{rev} the magnetization reversible and M_{an} the magnetization anhysteretic. In equation (1) $\kappa=k/\mu_0$ is expected as the pinning coefficient κ will be in units of A/m, δ is a directional parameter and takes the value ±1 according to dH /dt sign.

The Jiles-Atherton hysteresis model is based on the magnetization process. Its main advantage is that parameter determination is possible by using only one measured hysteresis loop, which involves important saturation [6] and can be adapted to dynamic phenomena consideration [3], [5]. However, it presents important drawbacks, such as difficult parameter identification processes, unphysical behavior of the model near loop tips and sometimes asymmetric and/or open loops at low fields [6]. The most important task of the Jiles-Atherton algorithm is to find, a theoretical hysteresis curve with known generating parameters α, α, c and κ. These parameters and the saturation magnetization M_s are the five model parameters which have to be determined from measured hysteresis characteristics. In the case of dynamic phenomena consideration [4], [5] a good compromise between calculation effort and precision can be obtained by using various differential susceptibilities through the following equations:

$$\left(\frac{dM_{an}}{dH}\right)_{M=0H=0} = \chi'_{an} = \frac{M_S}{3\alpha - aM_S} \tag{3}$$

$$\left(\frac{dM}{dH}\right)_{M=0H=0} = \chi'_{in} = \frac{cM_S}{3\alpha_S} \tag{4}$$

$$\kappa = \frac{M_{an}(H_c)}{1-c} = \left\{a + \frac{1}{\chi'_{\max} - \frac{c}{1-c}\frac{dM_{an}(H_c)}{dH}}\right\} \tag{5}$$

Fig. 1 shows experimentally defined hysteresis loops for grain oriented Hi B 103H27 iron laminations under sinusoidal excitation of 50 Hz using Epstein device for different flux densities B. These curves have been used as basis to define parameters for the Jiles-Atherton model representation of iron losses.

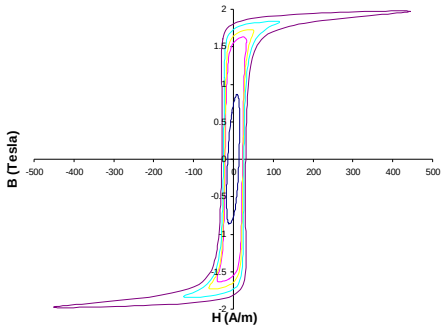

Fig. 1. Hysteresis Loops for the material Hi B 103H27, under various magnetic flux densities.

Table 1 presents power losses for different flux densities from experimental data for oriented Hi B 103H27. The experimental data were validated comparatively with manufacturer's data sheets. On the manufacturer's data sheets in Fig. 2 the corresponding measurement's points have been placed. The respective losses are in good agreement with the ones provided by the constructor of the laminations, as shown in Fig. 2.

Table 1.

Flux Density B (Tesla)	Power losses (W/kgr)
0.85	0.246675532
1.63	0.866134752
1.72	1.026374113
1.83	1.335549645
1.97	2.090203901

To set up the model, only one measured hysteresis loop is necessary in order to reach saturation. The tuning of model parameters has been performed by measuring iron lamination hysteresis loop under sinusoidal excitation. Fig. 3 shows the hysteresis loop with continuous line for grain oriented Hi B 103H27 measured for excitation frequency of 50 Hz. With dashed line shown the calculated loop based on Jiles – Atherton model. The respective model parameters are tabulated in Table 2.

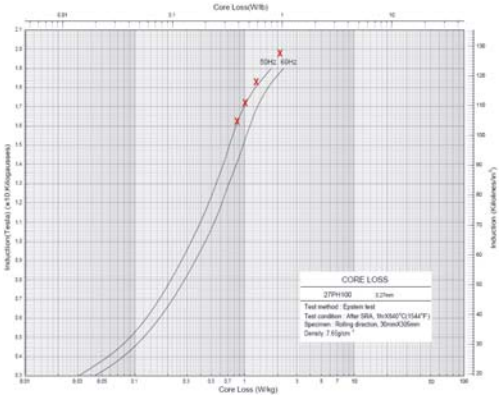

Fig. 2. Experimental validation of core power losses with respect to the constructional data.

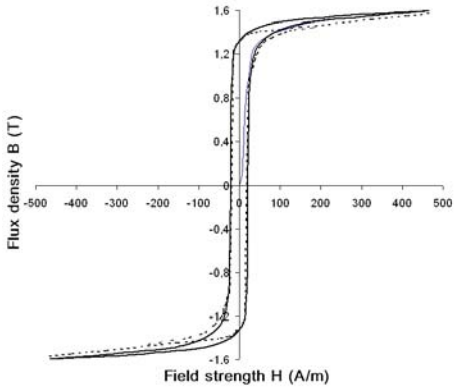

Fig. 3. Hysteresis loops in iron laminations under sinusoidal excitation at 50 Hz ——— : measured by the Epstein device - - - - : calculated Jiles-Atherton model.

Table 2.

α	490
k	1500
alpha	0,001
c	0,05

Fig. 4 show the experimental B-H loop for M4 material at 50 Hz for different flux densities B and in Table III the power losses in W/Kgr.

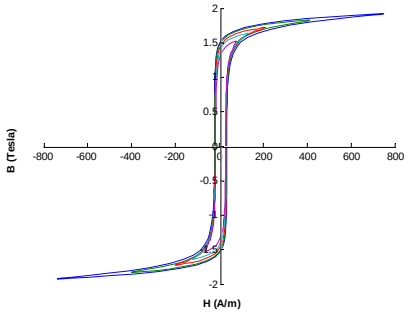

Fig. 4. Hysteresis Loops for the material M4, under various magnetic flux densities.

Table 3.

Flux Density B (Tesla)	Power losses (W/kgr)
0.85	0.246675532
1.63	0.866134752
1.72	1.026374113
1.83	1.335549645
1.97	2.090203901

Fig. 5 show a comparison of power losses between the materials HiB and M4 for excitation frequency of 50 Hz. We observe that M4 has more power losses than HiB for the same flux density.

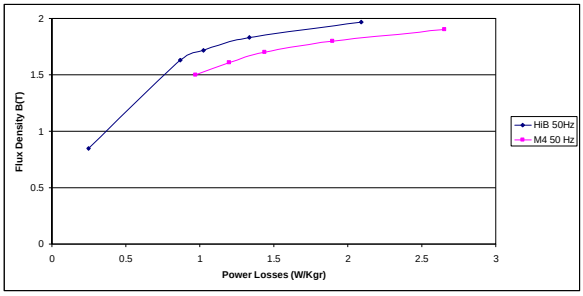

Fig. 5. Comparison of power losses between HiB and M4.

Hysteresis loops for the material M4 in various frequencies are presented in Fig. 6. Inner loop corresponds to 50 Hz, next one stand for 100 Hz measured loop, followed by 150 Hz and 250 Hz outer loop. All the measurements are for maximum flux density B = 1.7 Tesla. We observe the enlargement of hysteresis loops with the increase of frequency, as well as the increase of losses as it appears also in Fig. 7 where is presented a comparison of losses concerning the frequency.

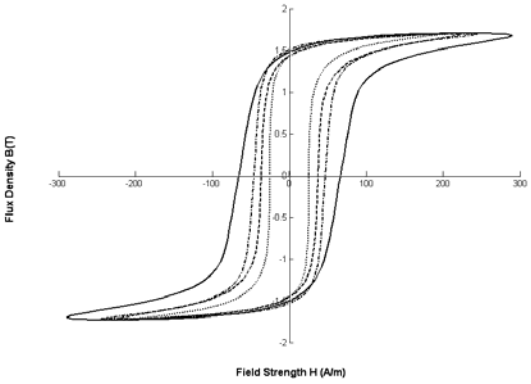

Fig. 6. Hysteresis Loops for the material M4, under various frequencies.

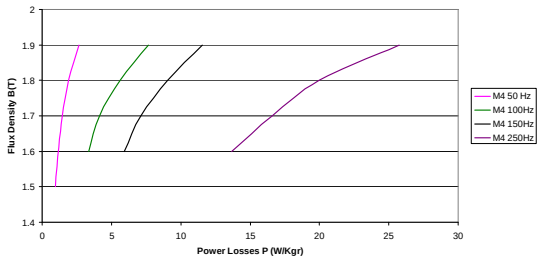

Fig. 7. Power Losses for M4 material in different frequencies.

3. Conclusions

The model parameters are determined from experimental data of hysteresis loops in Epstein device under sinusoidal excitation. The parameters variations with frequency provide acceptable accuracy in the evaluation of the area of hysteresis loops.

The discrepancy between experimental and theoretical data can be attributed to the fact that the maximum induction measured at higher frequencies by the Epstein device used, was limited due to the supply amplifier saturation resulting in a distortion of the imposed voltage waveform. It is well-known that Jiles-Atherton model gives less accuracy at low field values.

The respective losses are in good agreement with the ones provided by the constructor of the laminations, for the material Hi B 103H27and M4.

Acknowledgement

This work was supported in part by the General Secretariat for Research and Technology of Greece under PENED Grant No. 03ED045.

References

[1] D. C. Jiles, J. B. Thoelke, M. K. Devine, “Numerical Determination of Hysteresis Parameters for the Modeling of Magnetic properties Using the Theory of Ferromagnetic Hysteresis”, IEEE Transactions on Magnetics **28**(1), 27 (1992).

[2] G. Friedman, I. D. Mayergoyz, “Hysteretic energy losses in media described by vector Preisach model”, IEEE Transactions on Magnetics **34**(4), 1270 (1998).

[3] E. Cardelli, R. Giannetti, B. Tellini, “Numerical Characterization of Dynamic Hysteresis Loops and Losses in Soft Magnetic Materials”, IEEE Trans. on Magnetics **41**(5), 1540 (2005).

[4] D. C. Jiles, J. B. Thoelke, “Theory of Ferromagnetic Hysteresis: Determination of Model Parameters from Experimental Hysteresis Loops”, IEEE Transactions on Magnetics **25**(5), 3928 (1989).

[5] D. C. Jiles, “Frequency Dependence of Hysteresis Curves in «Non Conducting» Magnetic Materials”, IEEE Transactions on Magnetics **29**(6), 3490 (1993).

[6] Dieter Lederer, Hajime Igarashi, Arnulf Kost and Toshihisa Homma, “On the Parameter Identification and Application of the Jiles-Atherton Hysteresis Model for Numerical Modeling of Measured Characteristics”, IEEE Transactions on Magnetics **35**(3), 1211 (1999).

[7] P. Rovolis, A. Kladas, J. Tegopoulos, “Laminated iron core losses evaluation and measurements”, Journal of Materials Processing Technology **181**, 182 (2007).

*Corresponding author: panrov@mail.ntua.gr